

Richard Bussow

Einsteinufer 25, 10587 Berlin

Richard Bussow^y

(Dated: March 21, 2019)

The work addresses the definition of a wavelet that is adapted to analyse a flexural impulse response. The wavelet gives the opportunity to directly analyse the dispersion characteristics of a pulse. The aim is to localize a source or to measure material parameters. An overview on the mathematical properties of the wavelet is presented. An algorithm to extract the dispersion characteristics with the use of genetic algorithms is outlined. The application of the wavelet is shown in an example and experiment.

PACS numbers: 43.60 H j 43.60 Jn

I. INTRODUCTION

The wavelet transform is a promising method to evaluate the frequency dependent arrival time of a pulse in dispersive media. It can be used for the localization of sources and anomalies in a object^{1,2,3}. The underlying concept of this method will be briefly explained for a one-dimensional structure (e.g. a beam).

A fundamental difference between most waveforms in structures and fluids is the dispersion. A pulse propagating in a structure with the frequency dependent group velocity c_g changes its shape. Due to this dispersion the pulse is not recognizable with correlation techniques that can be useful in locating airborne sound sources.

The wavelet transform is very useful to extract exactly the arrival time t_a of a pulse in a dispersive media

$$t_a = x/c_g \tag{1}$$

The continuous wavelet transform L of a function y is

$$L y(a;b) = \frac{1}{c} \int_{-\infty}^{\infty} y(t) \frac{t-b}{a} dt \tag{2}$$

The analogue to the Fourier transform spectrogram is the scalogram defined as $\int y(a;b) f$. It can be shown that for a fixed scaling parameter a the arrival time t_a is the point in time where the maximum of the scalogram is present $\int y(a;t_a) f$. To locate a source one needs

1. the point in time the pulse occurred, the group velocity and a sensor, or
2. two sensors, or

3. one sensor measuring two distinguishable wave types⁴.

If the position of the source is known it is possible to extract material parameters⁵. To improve this method dispersion based transforms have been proposed⁶, which is based on a method called Chirplet transform^{7,8}.

Here a different for bending waves is presented. The underlying concept is not to measure the arrival time but to extract directly the dispersion of the pulse. The dispersion of the pulse is dependent on the distance between source and receiver. If it is possible to extract exactly this spreading of the pulse one has directly the distance or the material properties, depending on which is known. The velocity $v(x;t)$ resulting from the bending wave propagation for infinite plate of a force impulse $F_a(t) = F_0(t)$ at $r = 0$ is

$$v(r;t) = \frac{F_0}{4 t B^0 m^0} \sin \frac{r^2}{4 t} \tag{3}$$

where $D = \frac{E h^3}{12(1-\nu^2)}$, E the elastic modulus, h the plate thickness, ν the Poisson's ratio and m^0 the mass per unit surface area. The factor $D i = \frac{x^2}{4}$ is named dispersion number, which is a measure of the spreading of the different spectral fractions of the pulse. In the following a new adapted wavelet will be derived to extract the dispersion number from the measured pulse. Usually a wavelet is designed to localize a certain frequency. The proposed wavelet has a frequency range that is distributed over the wavelet length just like equation (3).

One may interpret the continuous Wavelet transform as a cross-correlation of y and f . The underlying concept is to find the function which is highly correlated with the impulse response. The difference is the role of the scaling parameter a . It is vital to produce the presented results to use the scaling parameter as it is defined in equation (2).

The dispersion number is determined by the scaling factor with the highest value of the scalogram. In principle

arXiv:physics/0611022v1 [physics.data-an] 2 Nov 2006

Institute of Fluid Mechanics and Engineering Acoustics, Berlin University of Technology
^yURL: <http://www.tu-berlin.de/fb6/ita>

this can be done with a fine grid of (a;b) values. A more efficient way is to use an optimisation scheme. Gradient based optimisation is not reliable in finding a global optimum. A second problem is the localisation of several overlapping pulses. A popular method that is able to fulfil these requirements are genetic algorithms.

II. BENDING WAVELET

Several different definitions based on the Morlet wavelet and the Chirplet transform^{7,8} have been investigated. For brevity an extensive discussion about the different efforts is omitted. The details of the mathematical background of the wavelet transform can be found in the literature^{9,10}.

The section begins with the definition of a wavelet with compact support and zero-mean. It follows a comment on the amplitude and frequency distribution and ends with possible optional definitions.

A. Definition

A wavelet must fulfil the admissibility condition

$$0 < c = 2 \int_1^{\infty} \frac{|\hat{\psi}(\omega)|^2}{\omega^2} d\omega < 1; \quad (4)$$

where $\hat{\psi}(\omega)$ is the Fourier transform of the wavelet. The proposed wavelet has a compact support $(t_{min}; t_{max})$, which means that the admissibility condition is fulfilled if

$$\int_{t_{min}}^{t_{max}} \psi(t) dt = 0 \quad (5)$$

holds. The mother wavelet is

$$\psi(t) = \begin{cases} \frac{\sin(\omega t)}{t} & \text{for } t_{min} < t < t_{max} \\ 0 & \text{otherwise} \end{cases}; \quad (6)$$

called bending wavelet. To fulfil the admissibility condition t_{min} and t_{max} are defined so, that equation (5) holds. With the integral-sine function $Si(x) = \int_0^x \sin(t) dt$ one finds that

$$\int_{t_{min}}^{t_{max}} \frac{\sin(\omega t)}{t} dt = Si\left(\frac{\omega t_{max}}{t_{min}}\right) - Si\left(\frac{\omega t_{min}}{t_{min}}\right); \quad (7)$$

Since $\lim_{t \rightarrow 0} Si(t) = 0$ and that the Si-function for $t > 2\pi$ oscillates around $\pi/2$, one is able to choose t_{min} and t_{max} so, that

$$Si(\omega t_{min}) = Si(\omega t_{max}) = \pi/2; \quad (8)$$

This is a very easy option to define a wavelet and it will be used later to define similar wavelet. Equation

(8) can only be solved numerically so a good approximation should be used that leads to a simple expression for c . The support of the wavelet is defined by

$$\frac{1}{t_{min} - t_{max}} = \frac{(2n_{max} - 1)\pi}{2}; \quad (9)$$

The function $Si(\omega t)$ and proposed possible values of t_{min} or t_{max} are plotted in figure 1. In the worst case for $t_{max} = 2\pi$ and $t_{min} = \pi$ the difference in equation (5) is around 0.2, but for higher values of n_{min} their magnitude is in the order of other inaccuracies, so that it should be negligible. Like the Morlet wavelet, which fulfills the admissibility condition for $\lim_{t \rightarrow 0} \omega t \neq 0$ the bending wavelet fulfills the admissibility for $\lim_{t \rightarrow 0} \omega t \neq 0$. The value of the

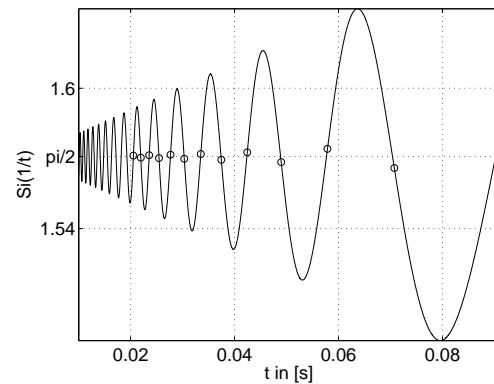


FIG. 1. $Si(\omega t)$ and circles at $\omega t = (2n - 1)\pi/2$

constant is calculated c with the norm in the Lebesgue space L^2 of square integrable functions

$$\|\psi\|_2^2 = \int_1^{\infty} |\hat{\psi}(\omega)|^2 d\omega = \int_1^{\infty} \frac{1}{\omega^2} d\omega = 1; \quad (10)$$

The integral in equation (10) is

$$\int_{t_{min}}^{t_{max}} \sin^2(\omega t) dt = \frac{1}{4} \left[\frac{2}{t_{min}} - \frac{2}{t_{max}} \right] \sin\left(\frac{2}{t_{min}}\right) + \sin\left(\frac{2}{t_{max}}\right); \quad (11)$$

With proposed choice of t_{min} and t_{max} the sine vanishes and a normalised $\|\psi\|_2^2 = 1$ wavelet is obtained if c is chosen to

$$c = \frac{1}{2} \left[\frac{1}{t_{min}} - \frac{1}{t_{max}} \right] = \frac{1}{2} (n_{max} - n_{min}); \quad (12)$$

B. Displacement-invariant definition

Wavelets that are defined by real functions have the property, that the scalogram depends on the phase of

the analysed function. Wavelets that are complex functions like e.g. the Morlet wavelet are called displacement-invariant. A wavelet $\psi_c(t) = \cos(t) + i \sin(t)$ that consists of a sine, $\sin(t)$ equation (6), and a cosine wavelet which is

$$\psi_c(t) = \begin{cases} \frac{\cos(1-t)}{t} & \text{for } t_{min} < t < t_{max} \\ 0 & \text{otherwise} \end{cases} \quad (13)$$

can be generalised. With the integral-cosine function $Ci(x) = \int_0^x \cos(t) dt$ one finds that

$$\int_{t_{min}}^{t_{max}} \frac{\cos(1-t)}{t} dt = Ci\left(\frac{1}{t_{max}}\right) - Ci\left(\frac{1}{t_{min}}\right) \quad (14)$$

The analogous definition of the value $\psi_c(2)$ for the Ci -function is

$$Ci(1/t_{min}) = Ci(1/t_{max}) = 0 \quad (15)$$

The approximation is given by

$$\frac{1}{t_{min} = m_{ax}} = n_{m_{ax} = m_{in}} \quad (16)$$

The effect is that the real- and the imaginary part of the resulting wavelet do not share the same support. This is a awkward definition but the difference between the two supports is rather small if the same value for $n_{m_{ax} = m_{in}}$ is used. To keep things simple only the real-valued sine wavelet is used in following.

C. Orthogonality of the bending wavelet

The trigonometric functions that are used for the Fourier transform establish an orthogonal base. Hence, the Fourier transform has the convenient characteristic that only one value represents one frequency in the analysed signal. Every deviation of this is due to the windowing function that is analysed with the signal. A ready the short time Fourier transform is not orthogonal, if the different windows overlap each other. Because of this overlap the continuous wavelet transform can not be orthogonal. The proposed wavelet should still be investigated since it is instructive for the interpretation of the results. The condition for a orthogonal basis in Lebesgue space L^2 of square integrable functions is

$$\int_1^Z \psi_j \psi_k = \delta_{jk} \quad (17)$$

Two different wavelets $\psi_j \psi_k$ can be build by using different scaling parameters a and/or different displacement parameters b . Here the effect of two scaling parameters is investigated, so the following integral is to be solved

$$\int_1^Z a_j a_k \sin(a_j t) \sin(a_k t) dt \quad (18)$$

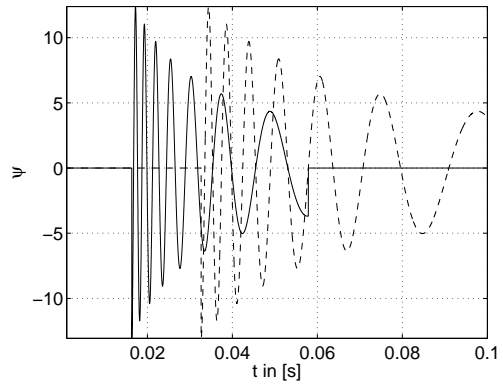


FIG. 2. Bending wavelet (6) for $a_1 = 1$ (solid) and $a_2 = 2$ (dashed), $n_{min} = 4$ and $n_{max} = 12$

To illustrate the integral two different versions of the wavelet are plotted in figure 2.

One finds that

$$\int_1^Z a_j a_k \sin(a_j t) \sin(a_k t) dt = \frac{a_j a_k}{a_k^2 a_j^2} a_j \cos\left(\frac{a_j}{t}\right) \sin\left(\frac{a_k}{t}\right) - a_k \cos\left(\frac{a_k}{t}\right) \sin\left(\frac{a_j}{t}\right) \Big|_{t_{min}}^{t_{max}} \quad (19)$$

The sine term in equation (19) vanishes since $t_{min} = m_{ax}$, also scale with a , but actually there are two different values of a and so not all four sine terms vanish. With this result one expects a rather broad area in $(a; b)$ with high values of the scalogram.

D. Time amplitude/frequency distribution

The time frequency distribution of the wavelet for a certain scaling factor a is determined by the argument of the sine function. The actual frequency of the wavelet is given by

$$f(t) = a = t^2 \quad (20)$$

The $1=t$ leading term affects the amplitude of the wavelet. Usually it is desired that the whole signal contributes linearly to the transform. To achieve this it is useful to have an amplitude distribution over time of the wavelet that is reciprocal to the amplitude distribution of the analysed signal. Since the bending wavelet has the same amplitude distribution as equation (3) this may lead to stronger weighting of the early high frequency components of the impulse response.

A force impulse that compensates the amplitude distribution of the impulse response follows a $1=t^2$ dependence.

III. CONTINUOUS WAVELET TRANSFORM WITH THE BENDING WAVELET

The application in the given context is to extract precisely the scaling factor with the highest value. How this is achieved will be discussed in the next section. Nevertheless, the realisation of a transform will be illustrative. The algorithm implementing the continuous wavelet transform with the bending wavelet can not be the same as the algorithm implementing a transform with any continuous wavelet, like the Morlet wavelet. The bending wavelet has a compact support, which must be defined prior to the transform. This can be done with an estimation of the frequency range and the dispersion number. With the equations (9) and (20) it holds that

$$n_{m_{ax}} = \text{oor} \left(\frac{r \frac{D i f_{m_{ax}}}{2} + \frac{1}{2}}{1} \right) ;$$

$$n_{m_{in}} = \text{ceil} \left(\frac{r \frac{D i f_{m_{in}}}{2} + \frac{1}{2}}{1} \right) ; \quad (21)$$

where $\text{oor}(\)$ rounds down towards the nearest integer and $\text{ceil}(\)$ rounds up. The knowledge of a useful frequency range should not provide any problems. But to know before which dispersion number will dominate the result is rather unsatisfactory. A more practical solution is to calculate the corresponding n -value within the algorithm, which is a easy task since $a = D i$. The problem with this possibility is that the support of the wavelet changes within the transform. Since the support is part of the wavelet this means that strictly one compares the results of two different wavelets. Since the wavelet is normalised the effect is rather small, but nevertheless it should be interpreted with care.

A. Example

To illustrate the use of the proposed wavelet the following function is transformed

$$y(t) = \begin{cases} t \sin(a=t); & \text{for } t_{m_{in}} < t < t_{m_{ax}} \\ 0 & \text{otherwise,} \end{cases} \quad (22)$$

with $a = 10$. The sampling frequency is $f_s = 2^9$, $t_{m_{in}}$ and $t_{m_{ax}}$ are defined by the corresponding values of $f_{m_{ax}} = f_s = 8$ and $f_{m_{in}} = 4$, for convenience the point $t = t_{m_{in}}$ is shifted to 10 t . The example function equation (22) is plotted in figure 3.

The example function is transformed with the algorithm that calculates $n_{m_{in}}$ and $n_{m_{ax}}$ with the corresponding value of $f_{m_{ax}}$, $f_{m_{in}}$ and a . The choice of the frequency range is critical, if it is too small information will be lost and if it is too big the parts that overlap the pulse may distort the result. Here the same frequency range as the analysed function is used.

The resulting scalogram is not plotted directly against the factor b , but shifted with the value of $t_{m_{in}}$. So

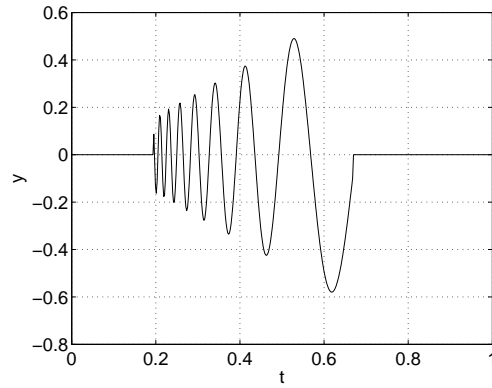


FIG. 3. A analysed example function (22)

the maximum value is at 10 t (figure 4), which is the value of t where $f_{m_{ax}}$ is located. The maximum value is shifted when $f_{m_{ax}} = f_s = 12$ is used, as can be seen in figure 5.

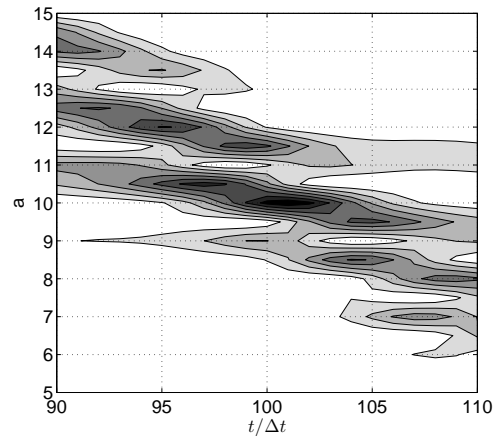


FIG. 4. Contour plot of the scalogram build with the bending wavelet transform of equation (22) with $f_{m_{ax}} = f_s = 8$ and $f_{m_{in}} = 4$

One may recognise that there are very high values if the wavelet is shifted and scaled along the curve $a=t$. This is expected theoretical, in section II.C, and can be interpreted descriptive since the wavelet does not localize one frequency, but has a wide frequency range that spreads over time. It can be quantified with equation (17). Evaluating this integral numerically for the values of $a_1 = 10$, $a_2 = 11.75$ and $b_2 = 7 t$ results in value of 0.68, which means that the peak at $a_2 = 11.75$ has 68% of the peak at $a_1 = 10$.

This problem of non-orthogonality is addressed by the following algorithm. The pulse is extracted from the signal by first locating the position t_{start} in the signal, where $f_{m_{ax}}$ has its maximum. This is done by a Morlet wavelet

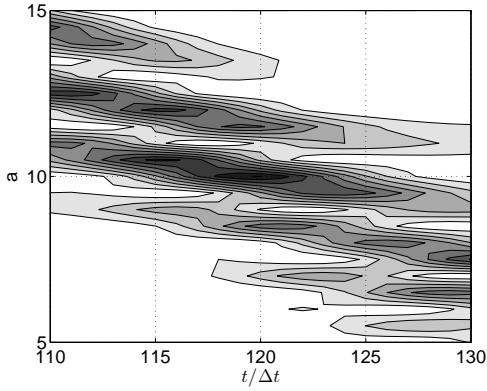


FIG . 5. Contour plot of the scalogram build with the bending wavelet transform of equation (22) with $f_{m \text{ ax}} = f_s=12$ and $f_{m \text{ in}} = 4$

transform with which one may find the value of t_{start} that has the highest value of $f_{m \text{ ax}}$. Now the transform with the bending wavelet is only done in the vicinity of t_{start} . Technically the displacement parameters are defined with t_{start} .

IV. LOCALIZATION WITH A GENETIC ALGORITHM

Genetic algorithms (GA) are a particular class of evolutionary algorithms that use techniques inspired by evolutionary biology such as inheritance, mutation, selection, and crossover. Genetic algorithms are categorized as global search heuristics. For details of the method please refer to the extensive literature, e.g.¹¹.

The genetic algorithm is chosen, since it is usually very reliable in finding a global optimum and its ability to find Pareto optimums to locate several pulses. However the drawback is the slow convergence, that can be improved with a local search method. Recent publications in the given context are^{12,13}.

The implementation is done with functions provided by the open source Matlab toolbox¹⁴, if not stated otherwise. Principally possible but not used in the example is the localization of two pulses that are overlapping. For the sake of brevity a discussion on how this can be achieved will be omitted. The algorithm works with two variables, displacement parameter and scaling factor of the bending wavelet.

The displacement parameter is defined by $t_{\text{start}} = 2$ or smaller values this depends on the size of the Morlet wavelet. For discrete functions it is an integer value, but nevertheless implemented as a floating point number, because of lacking support for such a combination in the toolbox. This fact is taken into account when calculating the wavelet transform. The following pseudo-code describes the genetic algorithm:

```

Linear distributed initial chromosome of t and a.
Bending wavelet transform with the initial chromosome.
Assignment to the current population.
Repeat
  Self-written rank based fitness assignment (current pop.).
  Selection with stochastic universal sampling.
  Recombination with the extended intermediate function.

```

```

Real-value mutation with breeder genetic algorithm.
Bending wavelet transform with the selected chromosome.
Self-written fitness based insertion with 70% new individuals.
Until max number of generations

```

In the end only the best individual is extracted. The algorithm is usually quite reliable. Nevertheless, since it is a stochastic method, it can be beneficial to restart the whole process or to work with several sub-populations.

A. Example

As an example the already transformed equation (22) is investigated. The frequency range is the same as the example plotted in figure 5. As a first step the value t_{start} is calculated with a Morlet wavelet transform at $f_s=12$. The result is plotted in figure 6, the maximum is at $t_i = 122$. From figure 5 one may conclude that the correct value is 120 this slight deviation is due to the fact that the Morlet wavelet has a rather broad frequency resolution and the amplitude of the signal is increasing with time. If the signal $\sin(a=t)=t$ is used the maximum is located at 118. The number of individuals is chosen to 100 the number of generations to 400.

The initial chromosome has a time index range of (106;138) which is $3=4$ and the range of the scaling factor is (5;15). The obtained scaling factor is $a = 9.99$. The frequency range of the bending wavelet is shorter than the values $f_{w \text{ max}} = 37.7 < 42.7 = f_s=12$ and $f_{w \text{ in}} = 4.756 < 4 < f_{m \text{ in}}$, this due to equation 21. The wavelet with the best scaling factor and the example function are plotted together in figure 7. One may recognize that the frequency-time distribution of both function match.

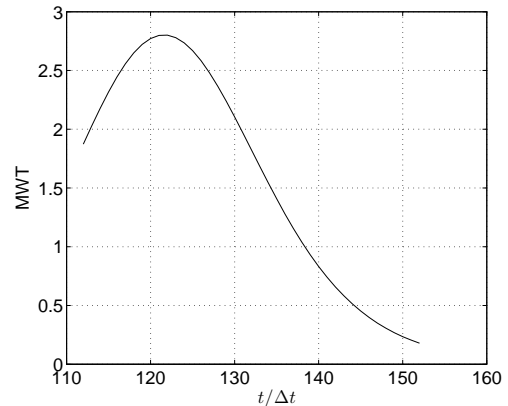


FIG . 6. Morlet wavelet transform of equation (22) with $f = f_s=12$

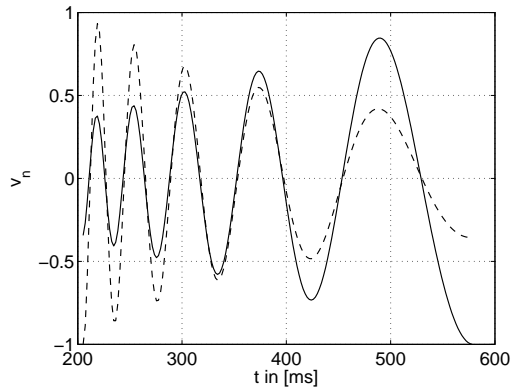


FIG . 7. B ending wavelet at $a = 9:99$ and the exam ple function

B . Experim ental results

The beam and the plate that were already investigated¹⁵ are analysed with the bending wavelet. The extracted dispersions numbers showed an agreement with the theoretical values within a deviation of only a few percent. This was the case for repeated measurements and different distances. Please refer to the figures 2 and 3 in¹⁵ for a plot similar to figure 7 for measured signals.

For the sake of brevity only a experiment with a time reversed pulse excitation of a beam is presented. The beam is clamped at one end and hanging on a twine on the other. Refer to figure 8 for a sketch of the setup.

The possibility of the excitation is theoretical predicted



FIG . 8. Sketch of the experim ental setup

in the prior publication¹⁵. The generation of the desired force excitation is done with a magnetic force transducer. The dispersion number for this pulse is chosen to $Di = 0:012$ with the given material properties of the beam the location of the pulse is at $x_{imp} = 0:6m$. The velocity is measured with a laser vibrometer in a distance of $x_{meas} = 1:13m$. The measured velocity is analysed with the bending wavelet and a maximum value of $Di = 0:00895$ is extracted within a frequency range between $f_{max} = 9:8kHz$ and $f_{min} = 1:1kHz$. The value of $x_m = 0:51m$ corresponds quite well with the theoretical value of $x_t = 0:53m$. The power spectrum over time is calculated with a Morlet wavelet transform and plotted in figure 9.

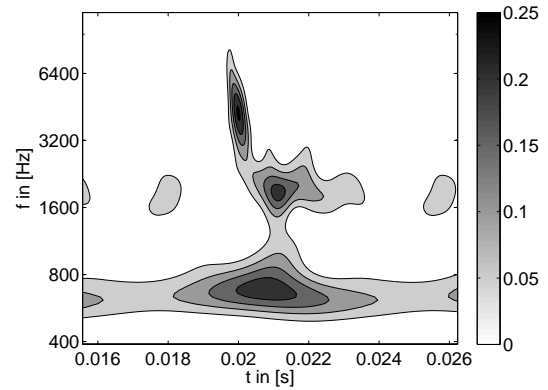


FIG . 9. Contour plot of the power spectrum over time obtained with the Morlet wavelet

V . CONCLUDING REMARKS

The definition of a new adapted wavelet is shown to be useful for analysing a external pulse response. It is possible

1. to obtain the distance of a pulse or the material properties with only one measurement,
2. to measure the material properties in a built in situation and
3. to analyse two overlapping pulse, which is not possible with the maximum of the Morlet wavelet transform where for each frequency one maximum value is extracted.

The accuracy and usability of the method seems to be promising. In the experiments a source could be localized with a deviation lower than 10% .

A precondition for the assessment is that the dispersion number is rather high and that the wave has a dispersion relation that follows a $\omega^2 \propto k^4$ dependence.

The choice of a useful frequency range can be problematic. It may be useful to first analyse the signal with a Morlet transform to find a useful range.

¹ H . Yamada, Y . Mizutani, H . Nishino, M . Takemoto, and K . Ono, " Lamb wave source location of impact on anisotropic plates", Journal of Acoustic Emission 18, 51{60 (2000).

² Y . Kin and E . Kin, " Effectiveness of the continuous wavelet transform in the analysis of some dispersive elastic waves", Journal of the Acoustical Society of America 110 (1), 86{94 (2001).

³ M . Rucka and K . Wilde, " Application of continuous wavelet transform in vibration based damage detection method for beams and plates", Journal of Sound and Vibration 297, 536{550 (2006).

⁴ J . Jiao, C . He, B . Wu, and R . Fei, " Application of wavelet transform on modal acoustic emission source location in

- thin plates with one sensor", *International Journal of Pressure Vessels and Piping* 81, 427{431 (2004).
- ⁵ Y. Hayashi, S. O gawa, H. Cho, and M. Takenoto, \Non-contact estimation of thickness and elastic properties of metallic foils by the wavelet transform of laser-generated lamb waves", *NDT & E international* 32/1, 21{27 (1998).
 - ⁶ J.C. Hong, K.H. Sun, and Y.Y. Kim, \Dispersion-based short-time fourier transform applied to dispersive waves", *Journal of the Acoustical Society of America* 117 (5), 2949{2960 (2005).
 - ⁷ S.M ann and S.Haykin, \The chirplet transform : A generalization of Gabor's logon transform ", *Vision Interface '91* 205{212 (1991).
 - ⁸ S.M ann and S.Haykin, \The chirplet transform : Physical considerations", *IEEE Trans. Signal Processing* 43, 2745{2761 (1995).
 - ⁹ S.M allat, *A wavelet tour of signal processing* (Academic Press) (1998).
 - ¹⁰ A.Louis, P.Maa , and A.Rieder, *Wavelets* (B.G.Teubner) (1994).
 - ¹¹ H.Pohlheim, *Evolutionare Algorithmen* (Springer) (2000).
 - ¹² C.Park, W.Seong, and P.Gerstoff, \Geoacoustic inversion in time domain using ship of opportunity noise recorded on a horizontal towed array", *Journal of the Acoustical Society of America* 117 (4), 1933{1941 (2005).
 - ¹³ L.Carin, H.Liu, T.Yoder, L.Couchman, B.Houston, and J.Bucaro, \Wideband time-reversal imaging of an elastic target in an acoustic waveguide", *Journal of the Acoustical Society of America* 115 (1), 259{268 (2004).
 - ¹⁴ A.Chippereld, P.Fleming, H.Pohlheim, and C.Fonseca, *The Genetic Algorithm Toolbox for MATLAB*, Department of Automatic Control and Systems Engineering of The University of Sheeld.
 - ¹⁵ R.Bussow, \Green's function for ex-ural in pulse response", (2006), URL <http://www.citebase.org/abstract?id=oai:arXiv.org:physics/06>